Wave-Based Attitude Control of Spacecraft with Fuel Sloshing Dynamics

J. W. Thompson[*], **W. J. O'Connor**[#],

School of Mechanical and Materials Engineering
University College Dublin
Belfield, Dublin 4, Ireland
[*] joseph.thompson@ucdconnect.ie
[#] william.oconnor@ucd.ie

ABSTRACT

Wave-Based Control has been previously applied successfully to simple under-actuated flexible mechanical systems. Spacecraft and rockets with structural flexibility and sloshing are examples of such systems but have added difficulties due to non-uniform structure, external disturbing forces and non-ideal actuators and sensors. The aim of this paper is to extend the application of WBC to spacecraft systems, to compare the performance of WBC to other popular controllers and to carry out experimental validation of the designed control laws. A mathematical model is developed for an upper stage accelerating rocket moving in a single plane. Fuel sloshing is represented by an equivalent mechanical pendulum model. A wave-based controller is designed for the upper stage *AVUM* of the European launcher *Vega*. In numerical simulations the controller successfully suppresses the sloshing motion. A major advantage of the strategy is that no measurement of the pendulum states (sloshing motion) is required.

1 INTRODUCTION

The failure of an early Jupiter ballistic missile in 1957 was caused by the interaction of the control system and the sloshing liquid fuel on board [1]. The problem was originally solved by aluminium drink cans, which could be fitted into the fuel tank and which floated on the surface of the fuel. Their friction both against the walls of the tank and against each other damped out the fuel oscillations. This experience motivated the eventual solution to the problem, which was the addition of baffles to the tank walls. However, baffles can only provide a certain level of damping of the liquid motion and can only be optimized for one tank fill level, so their effectiveness is reduced as the propellant is depleted. They also add complexity and mass to the vehicle and so increase costs. [2] It therefore becomes necessary to design a control system for a rocket which actively takes into account the effects of propellant sloshing and tries to compensate for them.

Many mechanical systems are inherently flexible, making it difficult to achieve rapid, controlled motion. The control challenge is even greater when the system is not well modelled, has dynamics that change with time, or is under-actuated.

A rocket with sloshing fluid propellant on board is an extreme case of such a system. A wave-based control method has been shown to cope well with the challenges outlined above [3, 4]. The key idea is that the motion of the actuator can be separated into two notional components, one travelling from the actuator into the system, the other leaving the system through the actuator. Intuitively the actuator simultaneously launches mechanical waves into a system while it absorbs returning waves. When the launching and absorbing is finished, vibrations have been damped and the desired reference motion is left behind. The method has been demonstrated to work well for 1-D and 2-D lumped flexible systems and in robotic and crane applications [5, 6].

The aim of this paper is to extend the application to the control of spacecraft with flexible structures and appendages (e.g. solar panels), and with on-board liquid propellant. This new area of application presents many new challenges. The spacecraft systems are often nonlinear, their associated flexibility is non-uniform, the sloshing dynamics are difficult or impossible to predict, and sensors and actuators can behave far from the ideal. In this paper the example of an accelerating upper stage rocket is examined.

2 MATHEMATICAL MODEL

In this section a mathematical model is developed for an upper stage accelerating rocket moving in a single plane. The rocket is assumed to be in a microgravity environment and free from aerodynamic effects. The sloshing fuel mass is represented by a mechanical analog in the form of a simple pendulum attached to the main rocket body. The fuel mass is partitioned, according to the tank fill level, into a fixed point mass and moving pendulum mass [7].

2.1 Planar upper stage model

The model of the upper stage rocket with single pendulum is shown in Fig. 1. The rocket body and pendulum are isolated and free body diagrams for each are shown in Fig. 2. The equations of motion for the two bodies may be written as:

$$F - R_x = ma_x \tag{1}$$

$$f - R_z = ma_z \tag{2}$$

$$I\ddot{\theta} = M + b(R_z) \tag{3}$$

$$R_x a \sin\phi + R_z a \cos\phi = 0 \tag{4}$$

$$m_f[a_x - b\dot{\theta}^2 + a\cos\phi(\dot{\theta}+\dot{\phi})^2 + a\sin\phi(\ddot{\theta}+\ddot{\phi})] = R_x \tag{5}$$

$$m_f[a_z - b\ddot{\theta} - a\sin\phi(\dot{\theta}+\dot{\phi})^2 + a\cos\phi(\ddot{\theta}+\ddot{\phi})] = R_z \tag{6}$$

All symbols for equations 1-6 are described in Tab. 1. Substituting for R_x and R_z from equations 5 and 6 into equations 1-4 eliminates these internal constraint

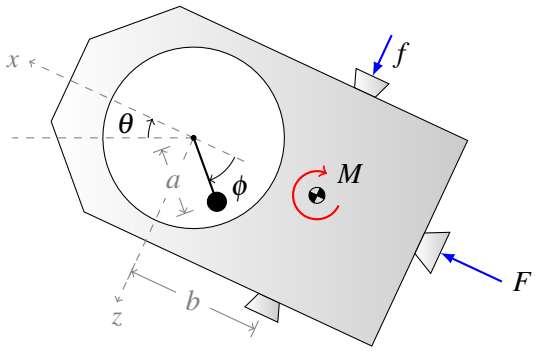

Figure 1: Upper stage rocket model

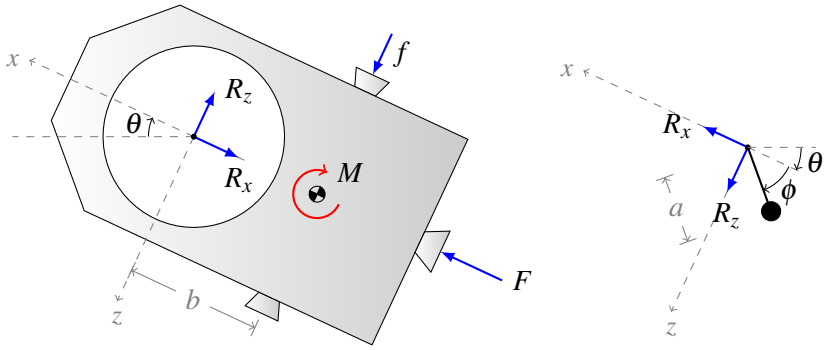

Figure 2: Free body diagrams

forces, and gives a minimal set of four equations for the four degree of freedom system.

$$(m+m_f)a_x - m_f b\dot{\theta}^2 + m_f a\cos\phi(\dot{\theta}+\dot{\phi})^2 + m_f a\sin\phi(\ddot{\theta}+\ddot{\phi}) = F \quad (7)$$

$$(m+m_f)a_z - m_f b\ddot{\theta} - m_f a\sin\phi(\dot{\theta}+\dot{\phi})^2 + m_f a\cos\phi(\ddot{\theta}+\ddot{\phi}) = f \quad (8)$$

$$(I+m_f b^2)\ddot{\theta} - m_f b a_z + m_f ab\sin\phi(\dot{\theta}+\dot{\phi})^2 - m_f ab\cos\phi(\ddot{\theta}+\ddot{\phi}) = M \quad (9)$$

$$(m_f a^2)(\ddot{\theta}+\ddot{\phi}) - m_f ab\sin\phi\dot{\theta}^2 - m_f ab\cos\phi\ddot{\theta} + m_f a(a_z\cos\phi + a_x\sin\phi) = 0 \quad (10)$$

2.2 Choice of actuators

The model described is general in that the body is actuated by two forces, F and f, and a moment, M. In reality the rocket may have one or many actuators, but in any configuration these actuators may be resolved into these two forces, axial and lateral, and a moment applied to the rocket body. In some cases

Table 1: List of symbols for equations 1-6

Symbol	Description
m	body mass
I	body moment of inertia
m_f	pendulum mass
a	length of pendulum
b	distance from COM to pivot point
θ	body pitch angle
ϕ	angle of the slosh pendulum w.r.t. body
F	axial force
f	lateral force
M	moment applied to body
R_x	internal constraint force at pivot point
R_z	internal constraint force at pivot point
a_x	axial body acceleration
a_z	lateral body acceleration

these inputs may not be independent of each other, but instead a function of some lesser number of inputs. For example, in the case of a rocket as shown in Fig. 3(a) with a single gimballed engine the forces and moment are no longer independent and are given by:

$$M = Tc\sin\delta, \quad F = T\cos\delta, \quad f = T\sin\delta \tag{11}$$

where T is the constant thrust developed by the rocket engine, c is the distance of the gimbal from the mass centre, and the single input is the engine gimbal angle δ. Similarly the rocket may be actuated by lateral thrusters as shown in Fig. 3(b). In this case:

$$M = T_l d, \quad F = T, \quad f = T_l \tag{12}$$

where again T is the constant thrust developed by the non-gimballed rocket engine, d is the axial distance from the thrusters to the mass centre, and the single input is the magnitude of the lateral thrust T_l.

2.3 Linearized model

Solving equations 7 and 8 for a_x and a_z respectively gives:

$$a_x = \frac{F + m_f b\dot{\theta}^2 - m_f a\cos\phi(\dot{\theta}+\dot{\phi})^2 - m_f a\sin\phi(\ddot{\theta}+\ddot{\phi})}{m+m_f} \tag{13}$$

$$a_z = \frac{f + m_f b\ddot{\theta} + m_f a\sin\phi(\dot{\theta}+\dot{\phi})^2 - m_f a\cos\phi(\ddot{\theta}+\ddot{\phi})}{m+m_f} \tag{14}$$

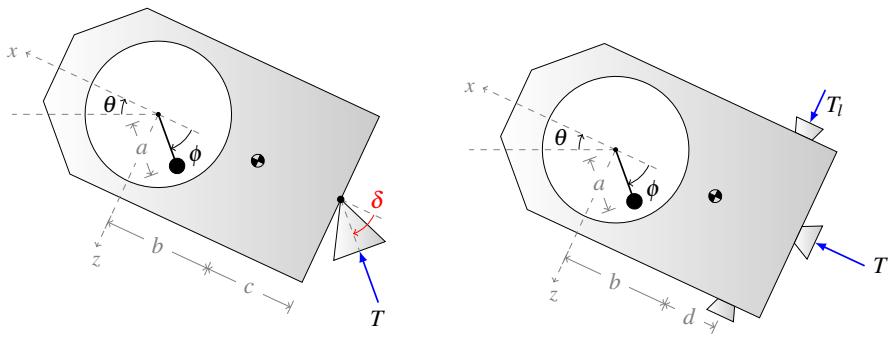

Figure 3: Possible actuator configurations

Substituting these expressions into equations 9 and 10 gives a simplified system of two equations describing the pitch and slosh dynamics:

$$[I + mm^\star(b^2 - ab\cos\phi)]\ddot{\theta} - mm^\star ab\ddot{\phi}\cos\phi + mm^\star ab(\dot{\theta}+\dot{\phi})^2\sin\phi = M + m^\star bf \tag{15}$$

$$m^\star(a^2 - ab\cos\phi)\ddot{\theta} + mm^\star a^2\ddot{\phi} + m^\star(aF - mab\dot{\theta}^2)\sin\phi = m^\star af\cos\phi \tag{16}$$

where:

$$m^\star = \frac{m_f}{m + m_f} \tag{17}$$

After linearization about $[\theta, \phi, \dot{\theta}, \dot{\phi}] = 0$ equations 15 and 16 become:

$$[I + mm^\star(b^2 - ab)]\ddot{\theta} - mm^\star ab\ddot{\phi} = M + m^\star bf \tag{18}$$

$$m^\star(a^2 - ab)\ddot{\theta} + mm^\star a^2\ddot{\phi} + m^\star aF\phi = m^\star af \tag{19}$$

The state vector of the linearized system consists of the pitch and slosh angles and their derivatives:

$$\mathbf{x} = [\theta, \phi, \dot{\theta}, \dot{\phi}]^T \tag{20}$$

It is assumed that the axial thrust F is a constant, so that the input vector consists of the lateral force f and moment M:

$$\mathbf{u} = [f, M]^T \tag{21}$$

Now equations 18 and 19 may be rewritten in state space form:

$$\dot{\mathbf{x}} = \mathbf{A}\mathbf{x} + \mathbf{B}\mathbf{u} \tag{22}$$

where:

$$\mathbf{A} = \begin{bmatrix} 0 & 0 & 1 & 0 \\ 0 & 0 & 0 & 1 \\ 0 & -\frac{Fbm_f}{I(m+m_f)} & 0 & 0 \\ 0 & -\frac{Fm_f(b^2-ab)}{Ia(m+m_f)} - \frac{F}{am} & 0 & 0 \end{bmatrix}, \quad \mathbf{B} = \begin{bmatrix} 0 & 0 \\ 0 & 0 \\ 0 & \frac{1}{I} \\ -\frac{1}{am} & \frac{(b-a)}{Ia} \end{bmatrix} \tag{23}$$

We find that the open-loop system ($\mathbf{u} = \mathbf{0}$) is aymptotically stable (all eigenvalues have negative real part) if and only if:

$$\frac{mm_f(b^2 - ab)}{m + m_f} + I > 0 \tag{24}$$

Possible pendulum configurations are shown in Fig. 4. For $b < 0$ (pendulum pivot point behind the mass centre) (Fig. 4(a)) or $b > a$ (whole pendulum in front of mass centre) (Fig. 4(b)) this condition is always satisfied, but in the region $0 < b < a$ stability is achieved only if:

$$a - b > \frac{I(m + m_f)}{bmm_f} \tag{25}$$

This is exacly equivalent to equation 24 and physically this means that the pendulum must straddle the point P shown in Fig. 4(c) which is a distance $-\frac{I(m+m_f)}{bmm_f}$ from the centre of mass along the x-axis.

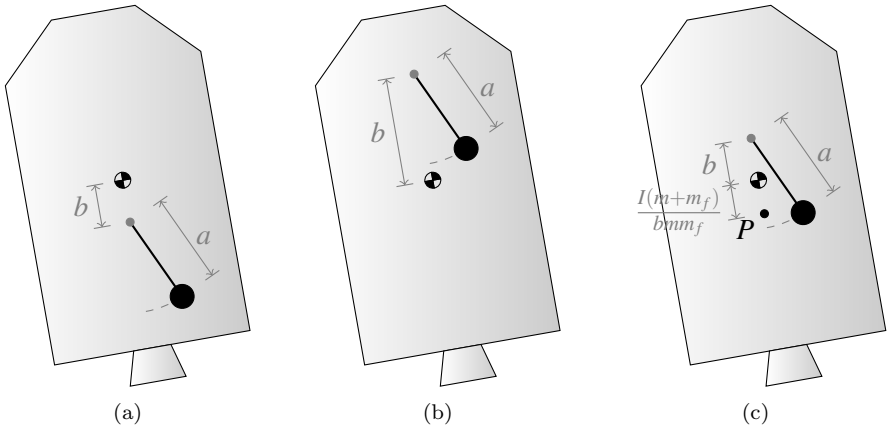

Figure 4: Possible pendulum configurations

3 WAVE-BASED MODEL

The first step in developing a wave model for the rocket system is to express the equations of motion in a form resembling a cascaded lumped flexible system. The rocket system described by equation 22 has two degrees of freedom and so it is required to transform this to appear like a 2-DOF lumped flexible system, i.e. two masses/inertias with an interconnecting spring. It is also required that there be a single control input which actuates just the first degree-of-freedom, i.e. a single launcher and absorber of waves. The system should have the following form:

$$\dot{\mathbf{z}} = \hat{\mathbf{A}}\mathbf{z} + \hat{\mathbf{B}}f_0 \tag{26}$$

where:

$$\hat{\mathbf{A}} = \begin{bmatrix} 0 & 0 & 1 & 0 \\ 0 & 0 & 0 & 1 \\ -\frac{k_1}{m_1} & \frac{k_1}{m_1} & 0 & 0 \\ \frac{k_1}{m_2} & -\frac{k_1}{m_2} & 0 & 0 \end{bmatrix}, \quad \hat{\mathbf{B}} = \begin{bmatrix} 0 \\ 0 \\ \frac{1}{m_1} \\ 0 \end{bmatrix}, \quad \mathbf{z} = \begin{bmatrix} x_1 \\ x_2 \\ \dot{x_1} \\ \dot{x_2} \end{bmatrix} \tag{27}$$

These equations describe the dynamics of a 2-DOF mass-spring system, where x_1 and x_2 are the displacements of the masses and f_0 is the actuating force on the first mass. Assume that the lateral force f on the rocket body is zero and just the pure moment M is available for control purposes. In reality this could be imagined as a gimballed rocket engine with lateral thrusters at mass centre to cancel the lateral forces from the engine. The input matrix B from equation 23 then becomes a column vector:

$$\mathbf{B} = \begin{bmatrix} 0 \\ 0 \\ \frac{1}{I} \\ \frac{(b-a)}{Ia} \end{bmatrix} \tag{28}$$

To transform the system to the required form the change of basis $\mathbf{z} = \mathbf{M}\mathbf{x}$ is used, where:

$$\mathbf{M} = \begin{bmatrix} 1 & 0 & 0 & 0 \\ 1 & \frac{a}{a-b} & 0 & 0 \\ 0 & 0 & 1 & 0 \\ 0 & 0 & 1 & \frac{a}{a-b} \end{bmatrix}, \quad \hat{\mathbf{A}} = \mathbf{M}\mathbf{A}\mathbf{M}^{-1}, \quad \hat{\mathbf{B}} = \mathbf{M}\mathbf{B} \tag{29}$$

The states are now:

$$x_1 = \theta, \quad x_2 = \theta + \left(\frac{a}{a-b}\right)\phi \tag{30}$$

and the parameters of the system are given by:

$$k_1 = \frac{Fbm_f(a-b)}{a(m+m_f)}, \quad m_1 = I, \quad m_2 = \frac{mm_f(b^2-ab)}{m+m_f} \tag{31}$$

Fig. 5 shows the equivalent mass-spring system with a notional mass m_0 and notional spring of stiffness k_0 appended to the system. The force in the first spring is considered to be the actuation force f_1. The system may now be considered as actuated by the displacement x_0 of notional mass m_0 such that:

$$f_0 = k_0(x_0 - x_1) \tag{32}$$

The wave model assumes that the displacement of each mass x_i is can be seperated into leftward and rightward travelling components a_i and b_i respectively or A_i and B_i in the Laplace (complex frequency) domain [8]. The propagation of the rightward and leftward travelling waves is described by wave transfer functions G_i, H_i and F respectively such that:

$$A_i = G_{i-1}A_{i-1}, \quad B_i = H_iB_{i+1}, \quad B_2 = FA_2 \tag{33}$$

For controller design it is easier to work with transfer functions that deal with the actuating force F_0 rather than the notional displacement X_0. The spring force F_0 can also be separated into rightwards and leftwards travelling components F_{0A} and F_{0B} respectively. Then the cross-over wave transfer functions P_0 and Q_0 relate displacements to forces by:

$$A_1 = P_0 F_{0A}, \quad F_{0B} = Q_0 B_1 \tag{34}$$

and these can be calculated from the ordinary wave transfer functions as:

$$P_0 = \frac{G_0}{k_0(1 - G_0)}, \quad Q_0 = k_0(H_0 - 1) \tag{35}$$

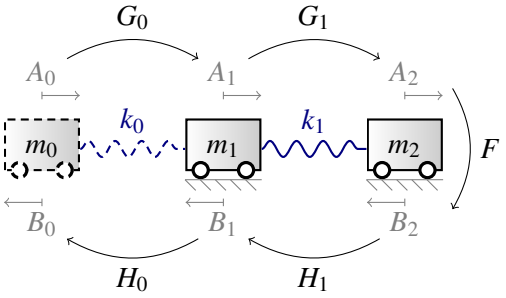

Figure 5: Wave model of the rocket

4 CONTROL DESIGN

4.1 Wave-Based Controller

A WBC3 (force actuated) controller was designed to control the rocket attitude θ. The controller uses only the transfer functions G_0 and H_0. The second-order uniform system approximations [8] are used where:

$$G_0 = \frac{\omega_G^2}{s^2 + \omega_G s + \omega_G^2}, \quad \omega_G = \sqrt{\frac{2k_0}{m_1}} \tag{36}$$

$$H_0 = \frac{\omega_H^2}{s^2 + \omega_H s + \omega_H^2}, \quad \omega_H = \sqrt{\frac{2k_0}{m_0}} \tag{37}$$

The wave-based control scheme is shown in Fig. 6. θ_{ref} is the desired reference pitch angle. The control input is the input torque M_{ref}. Two variables are measured for feedback. These are the pitch angle θ and the actual achieved torque M. In this paper the actuator is assumed ideal except for the saturation limits. The wave based control strategy launches a wave equal to half the

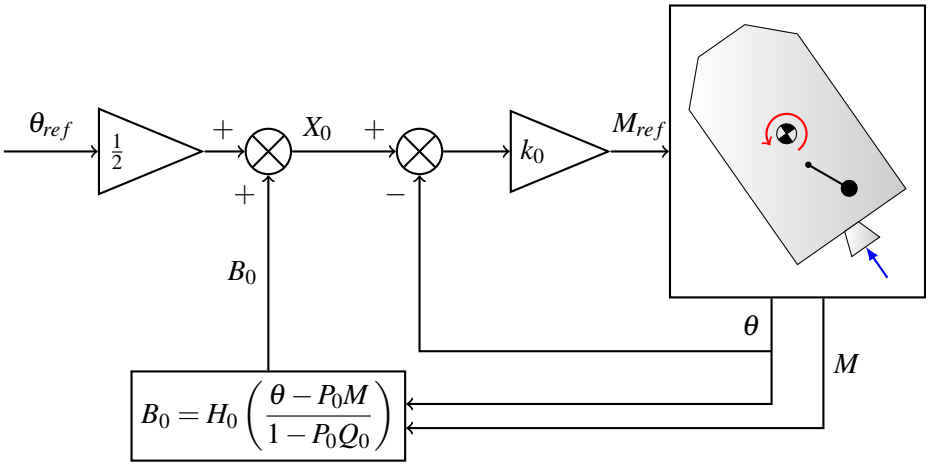

Figure 6: Wave-based control system

reference signal θ_{ref}. The measured values of θ and M are then used to calculate the returning wave component at the actuator which can be calculated as:

$$B_0 = H_0\left(\frac{\theta - P_0 M}{1 - P_0 Q_0}\right) \tag{38}$$

The actuator is then moved to match this returning wave component and thereby absorb it. When the absorbing is finished the system will have been displaced by twice the specified launch wave, i.e. will be at the reference displacement.

4.2 Time-Optimal Controller

For comparison, the torque-limited bang-bang solution for a rest-to-rest maneuver of a rigid rocket was calculated. With the slosh pendulum frozen in position the moment of inertia of the rocket body about the overall mass centre is given by:

$$I_{rigid} = I + \frac{m m_f (b-a)^2}{(m+m_f)} \tag{39}$$

The switching time for a rest to rest manoeuvre is:

$$t_s = \sqrt{\frac{\theta_{ref} I_{rigid}}{M_{max}}} \tag{40}$$

where M_{max} is the maximum torque. Then the control input for the bang-bang manoeuvre beginning at $t = t_0$ is:

$$M = \begin{cases} 0 & t < t_0 \\ M_{max} & t_0 < t < t_0 + t_s \\ -M_{max} & t_s < t < t_0 + 2t_s \\ 0 & t > t_0 + 2t_s \end{cases} \tag{41}$$

5 RESULTS

The wave-based controller was tested by numerical simulation. Suitable parameters for the presented rocket model were chosen to represent *AVUM*, upper stage of the European *Vega* launcher [9] (Tab. 2). The included slosh pendulum represents the primary sloshing mode for the rocket's fuel tank when half full. The saturation torque M_{max} was calculated from the maximum gimbal angle of the *AVUM* engine. The values chosen for notional mass and spring stiffness were $m_0 = m_1$ and $k_0 = k_1(\frac{m_1}{m_2})$, however, the choice for these parameters is arbitrary to some degree and a range of values will give a good control response. Results are shown in Fig. 7 for a five degree step change in commanded pitch angle θ_{ref}. The wave-based controller is compared to the torque-limited time-optimal solution for the rigidized rocket.

Table 2: Summary of model parameters representative of *AVUM* upper stage

Parameter	Value	Unit
m	2105	kg
m_f	88	kg
I	1883	$kg\ m^2$
a	0.53	m
b	-1.43	m
F	2450	N
M_{max}	931	$N\ m$

6 DISCUSSION

It can be seen that the fuel slosh dynamics cause the open-loop time optimal controller to land off target and drift away from the target over time. The fuel sloshing persists for long times in the absence of damping in the model. The wave-based controller lands on target and suppresses the sloshing motion. However, the sloshing persists for several oscillations. The reason for this is the non-uniformity of the system, i.e. unequal inertias m_1 and m_2. In this case m_1 is much less than m_2. From a wave perspective there is a change in wave impedance between the two different masses and some waves become trapped on

the right hand side of this boundary. For this reason the actuator only absorbs a fraction of the motion on each oscillation cycle, but over several cycles can absorb it all. When the ratio of inertias $\frac{m_1}{m_2}$ is much less than one, the effect of the pendulum on the body is much reduced and so it takes longer to fully suppress sloshing motions. This is acceptable, however, because in this case, by definition, the sloshing does not cause a major problem for the rocket controller. On the other hand, the control challenge is greatest when the fluid inertia ratio is large, and this is precisely when the new strategy delivers much improved performance. An interesting avenue of future research is developing wave-models and controllers which take into account the non-uniformity of the system to be controlled. A clear advantage of wave-based control is that all measuring is done at the actuator, in this case the rocket body, so no measurement of the pendulum states is necessary, which is a significant bonus given the challenge of measuring or modelling them in a real rocket. Future research includes making the controller robust to external disturbances such as aerodynamic, stage separation or gravity forces; considering non-ideal actuator and sensor behaviour; including multiple slosh pendulums representing either multiple fuel tanks or multiple modes of sloshing in a single tank; and extending the analysis to a 6-DOF model where roll, pitch and yaw must be simultaneously controlled.

References

[1] W. Haeussermann. Developments in the field of automatic guidance and control of rockets. *Journal of Guidance, Control, and Dynamics*, 4(3):225–239, May 1981.

[2] M. Reyhanoglu. Modeling and Control of Space Vehicles with Fuel Slosh Dynamics. 2004.

[3] William J O Connor. Excellent control of flexible systems. *Control*, pages 6181–6186, 2005.

[4] William O'Connor and Donogh Lang. Position Control of Flexible Robot Arms Using Mechanical Waves. *Journal of Dynamic Systems, Measurement, and Control*, 120(3):334, 1998.

[5] William J. O'Connor and Alessandro Fumagalli. Refined Wave-Based Control Applied to Nonlinear, Bending, and Slewing Flexible Systems. *Journal of Applied Mechanics*, 76(4):041005, 2009.

[6] William J. O'Connor. A Gantry Crane Problem Solved. *Journal of Dynamic Systems, Measurement, and Control*, 125(4):569, 2003.

[7] Franklin T Dodge. the New "Dynamic Behavior of Liquids in Moving Containers". *Southwest Research Institute*, 2000.

[8] William J. O'Connor. Wave-like modelling of cascaded, lumped, flexible systems with an arbitrarily moving boundary. *Journal of Sound and Vibration*, 330(13):3070–3083, 2011.

[9] Edouard Perez. Vega User's Manual, Issue 3, Revision 0. (3):188, 2006.

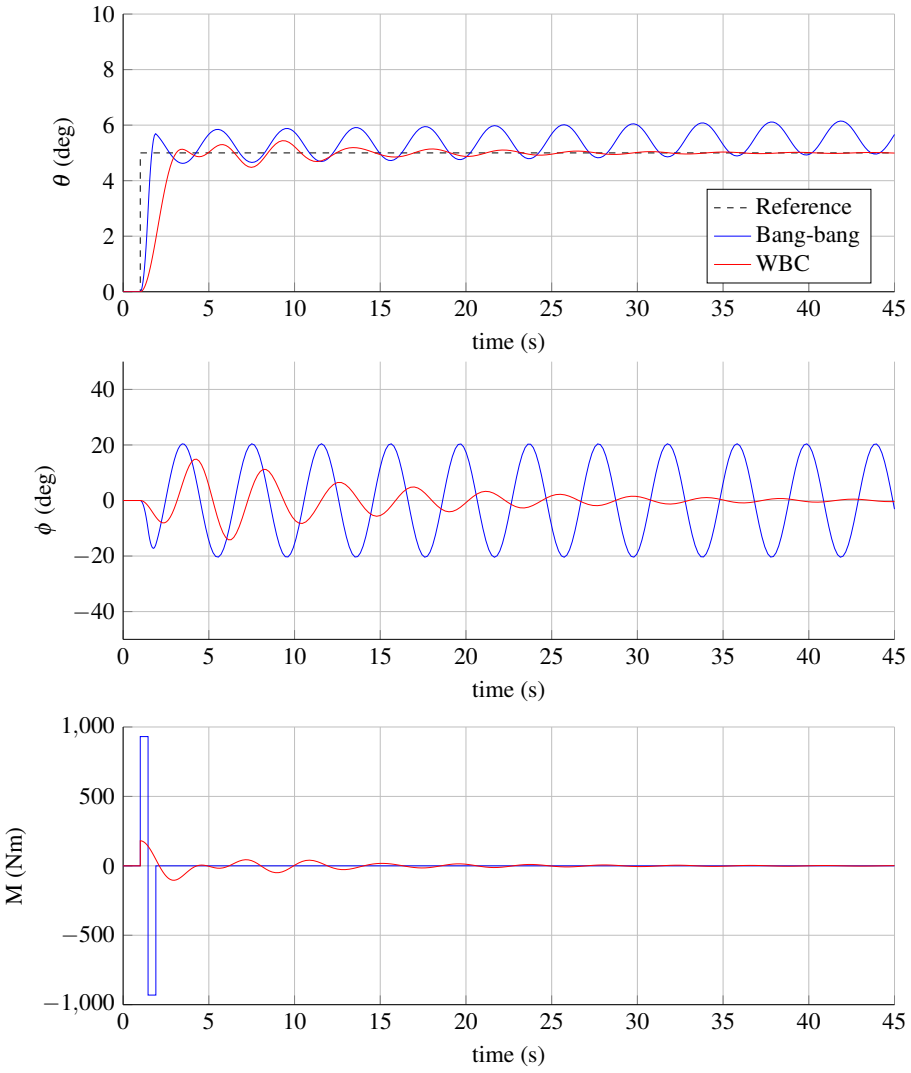

Figure 7: Pitch θ and pendulum angle ϕ for a 5 degree step change in θ_{ref}.